JOURNAL OF GEOPHYSICAL RESEARCH, VOL. 113, D07106, doi:10.1029/2007JD009027, 2008

An electric force facilitator in descending vortex tornadogenesis

Forest S. Patton,[1] Gregory D. Bothun,[1] and Sharon L. Sessions[2]

Received 30 May 2007; revised 16 November 2007; accepted 21 December 2007; published 9 April 2008.

[1] We present a novel explanation of the physical processes behind one type of cloud and ground-level tornadogenesis within a supercell. We point out that the charge separation naturally found in these large thunderstorms can potentially serve to contract the preexisting angular momentum through the additional process of the electric force. On the basis of this, we present a plausible geometry that explains why many tornado vortices begin at storm midlevel and build downward into ground-level tornadoes. A simple model based on this geometry is used to demonstrate the strength of the electric force compared to the required centripetal acceleration to maintain cloud midlevel tornado vortices measurable as tornado vortex signatures (TVSs). Furthermore, a model based on this geometry is used to get a time estimate for tornado vortex formation. From this we are able to identify a plausible value for the threshold charge density that would lead to tornadogenesis and tornado maintenance on the timescale of a few minutes. We show that the proposed geometry can explain the observations that ground-level tornadoes thrive in regions with high shear and large convective available potential energy (CAPE) and are able to make some predictions of specific measurable quantities.

Citation: Patton, F. S., G. D. Bothun, and S. L. Sessions (2008), An electric force facilitator in descending vortex tornadogenesis, *J. Geophys. Res.*, *113*, D07106, doi:10.1029/2007JD009027.

1. Motivation

[2] Many of the physical conditions required to initiate tornadoes are well understood on a broad qualitative level but many quantitative details remain unknown. On the qualitative level, it is apparent that the deep rotation of a supercell thunderstorm along with a buoyant updraft and a rain-driven downdraft create a probable environment for tornadogenesis. Yet, we still do not quantitatively understand the full range of energy inputs which allow particular storms to spawn tornadoes while other storms with similar macroscopic properties do not. Furthermore, we cannot currently predict the length (minutes to hours) or intensity of the tornadoes that do form [*Davies-Jones et al.*, 2001]. This suggests the presence of one or more physical thresholds in the system that, once exceeded, can spawn a tornado. Systems in which the relevant threshold is not achieved, therefore fail to form a tornado. As an example, evidence indicates that a certain amount of boundary layer shear in conjunction with a certain level of convective available potential energy (CAPE) is required for a tornado to occur [*Rasmussen and Blanchard*, 1998].

[3] One clear attribute is that most tornadoes spawn from supercells and associated convective activity. In particular, *Trapp et al.* [2005] showed that 79% of all measured tornadoes for the years 1998–2000 came from supercells. We also know that around two thirds of this 79% of supercell-spawned tornadoes begin their rotation aloft (2–7 km) and then descend to form ground-level tornadoes in what is measured as a descending TVS [*Trapp et al.*, 1999]. This means that roughly half of all the sampled tornadoes began their intense rotation high in a supercell cloud and then built downward to make ground-level tornadoes. This suggests the existence of a cloud-level triggering mechanism which we explore in this paper.

[4] While current theories adequately take into account the large-scale rotation and potential buoyancy associated with a supercell (see *Davies-Jones et al.* [2001] for a review) they do not yet include any effects from the substantial amounts of energy stored in charge separation. In this paper we link the contraction of preexisting angular momentum beginning in the heart of the supercell with an electrical force that naturally exists in all supercells because of charge separation. We qualitatively show how this embryonic tornado structure, enhanced by its electrical properties, can lead to a central downdraft that will build the contraction of rotation downward. We will then present a comparison model of required centripetal acceleration to that provided by the electric force. We will also use a simple model to demonstrate that the timescales associated with the development of the tornado are similar to empirical observation (e.g., minutes). We finish by theorizing how the downward building tornado vortex can instigate the release of latent heat and couple with preexisting boundary layer shear to lead to the formation of a stable ground-level tornado.

[1] Department of Physics, University of Oregon, Eugene, Oregon, USA.
[2] Department of Physics, New Mexico Institute of Mining and Technology, Socorro, New Mexico, USA.

0148-0227/08/2007JD009027$09.00

2. History

[5] As the large-scale lightning/thunder associated with supercells is clearly due to massive amounts of charge separation, the basic idea of charge exchange and movement having some bearing on tornadic activity has precedent. *Lucretius* [1950] and *Bacon* [1844], observing that lightning sometimes precedes a tornado, wrote about the idea in 60 BC and 1622, respectively. Later, *Peltier* [1840] and *Hare* [1837] independently put forth theories that tornadoes are conduits for charge exchange in the atmosphere. The quantitative ability to accurately measure the electrical properties of thunderstorms let alone tornadoes (e.g., charge densities, charge separation length scales, etc) did not exist when these theories were presented. This observational deficiency caused the subsequent neglect of these theories.

[6] *Vonnegut* [1960] revived the idea by hypothesizing that electrical heating (through ohmic dissipation) might be able to sustain the intense winds observed in a tornado. He conjectured that electrical heating from a continuous electrical current could create temperature gradients strong enough so that air would be accelerated to tornadic speeds. *Watkins et al.* [1978] later undertook a laboratory experiment which showed that a vortex discharge alone could not account for total tornado wind intensity; there was simply not enough current energy density in a thunderstorm to maintain the required constant arc.

[7] We agree that *Vonnegut's* [1960] theory is quantitatively untenable because of the huge amount of continuous current required to make it work. Qualitatively, however, there is certainly energy associated with the electrical field in supercells and the conversion of that energy into other forms may be one of the triggers or threshold mechanisms that spawn tornadoes. The observation that 79% of all tornadoes come from supercell thunderstorms, the largest and most intense class of thunderstorms, clearly suggests a connection. Furthermore, there are significant observations that link electrical activity to tornadoes.

3. An Electrical Connection

[8] Numerous eyewitness accounts within the last 100 years report various noteworthy electrical phenomena associated with tornadoes including St. Elmo's fire, glowing funnel, glowing patches of cloud, etc. *Church and Barnhart* [1979] compiled the eyewitness reports from 67 separate tornadoes between 1787 and 1975 into one paper. Despite their quantity, eyewitness reports are not quantitative and therefore do not provide conclusive proof of an electrical phenomenon. The eyewitnesses are not trained scientists, and this provides further grounds to question their testimony. The shear number of independent reports does, however, point to some sort of association between tornadoes and luminous electrical phenomena which is worthy of further investigation.

[9] Visual evidence and supporting eyewitness accounts of luminous electrical phenomena were presented by *Vonnegut and Weyer* [1966]. Their evidence was a nighttime picture that showed what appeared to be two glowing funnels at the approximate position where a tornado passed. Eyewitnesses also reported that the funnels were glowing and told of other electrical activity near the funnels.

[10] Further evidence of electrical activity associated with tornadoes has been collected in numerous studies in the form of electromagnetic (EM) noise called sferics [see *MacGorman and Rust*, 1998]. These high-frequency EM emanations are traditionally related to lightning and come in pulses coincident with lightning discharges. Both before and during a tornado remarkably intense sferics have been observed. During the lifecycle of the tornado the sferic pulse repetition rate becomes so high as to be almost constantly emitted. Sferic data suggests that in about 80% or more of tornadic storms there is an increase in total sferic rates near the time of the tornado [*MacGorman et al.*, 1989]. Furthermore, sferics with frequencies above 1 MHz were found to increase in intensity and become most extreme in the time leading up to and during a ground-level tornado [*MacGorman et al.*, 1989]. At the very least, this suggests some form of increase in total electrical activity within the system prior to and during a ground-level tornado. Observed radiation during tornadoes seems to indicate that a semicontinuous mode of lightning is occurring. *MacGorman et al.* [1989] suggested that the increase in the measured sferic intensities is dominated by intracloud lightning; this is similar to what has been observed recently in what are called lighting holes.

[11] Lightning holes are essentially lightning free regions within supercells that have been observed in association with strong updrafts (bounded weak echo regions) [*Lang et al.*, 2004]. They are identifiable because they occur in the deepest part of the thunderstorm surrounded by vigorous lightning. "Lightning holes . . . appear to be a characteristic signature of the impending occurrence or potential for occurrence of a tornado" [*Krehbiel et al.*, 2002, p. 3]. Some proof of this comes from the 29 June 2000 tornadic storm. A lightning hole was documented in the elevations between ~1.5 and 15 km directly above a ground-level tornado; the lightning hole appeared before tornado touchdown and became the most pronounced during the tornado [*Zhang et al.*, 2004]. Furthermore, *Zhang et al.* [2004, p. 624] found that "The lightning channels of intercloud lightning discharge exhibit clockwise rotary structures and do not have clear bilevel structures in the vicinity of the tornado." This phenomenon may support a charge relaxation mechanism possibly facilitated by tornadic activity that is not yet well understood.

[12] Overall, there seems to be appreciable evidence to indicate that there is a heightened level of electrical activity associated with and in the vicinity of tornadoes. From the sferic data and the lightning hole measurements there seems to be electrical activity preceding and concurrent with a ground-level tornado. Other authors [*Vonnegut*, 1960; *Winn et al.*, 2000] have compiled other electrical facts not mentioned in this paper. Motivated by such evidence for a more direct electrical connection, we will now propose a mechanism through which charged airflow aids in the organization of a tornado vortex measurable as a TVS and the subsequent development of a ground-level tornado.

4. Tornado Vortex Signature

[13] A TVS is a low-resolution Doppler radar image of an embryonic or fully developed tornado vortex. This observable radar image, which is evidence of strong axial rotation,

generally develops before a tornado touches down, intensifies while the tornado goes through its mature stage, and dissipates as the tornado dies [*Brown et al.*, 1978]. *Trapp et al.* [1999] found that roughly half of all tornado vortices are first measured aloft (median height of 4–5 km) and then build downward (mode I) while the other half either start near the ground and build upward quickly or form simultaneously over several kilometers of depth (mode II). Both modes are precursors to ground-level tornado formation but do not necessarily lead to tornadoes [*Trapp et al.*, 1999]. Likewise, a measurable TVS does not precede all tornadoes. *Davies-Jones* [1986] suggested that this might be due to limitations in radar resolution and/or the stringency of the automated detection algorithms. For simplicity, we will concentrate on mode I formation, but will touch on mode II a little as well.

5. Supercell Mesocyclone Charge Structure

[14] Initially, local weather conditions spawn a convective supercell. The defining characteristics of the supercell are large charge separations and a persistent large-scale rotation known as the mesocyclone. The spatial scale of this rotation is between 3 and 9 km in diameter [*Davies-Jones et al.*, 2001] and generally extends to the vertical limit of the storm [*MacGorman and Rust*, 1998, p. 236].

[15] Supercells are charge stratified, meaning that alternating regions of positive and negative charge layers are stacked on top of each other. *Stolzenburg et al.* [1998a] reported that supercell storms generally have 4 alternating charge layers in the strong updraft region and up to 8 layers outside the main updraft region. In the strong updraft region the lowest two layers consist of a deep (1–4 km), low-density positive charge region between about 4 and 8 km above mean sea level with a shallow, dense negative charge layer residing between 8 and 10 km above MSL. *Marshall et al.* [1995] were the first to report this phenomena and to note a very fast electric field change at the boundary between the lowest two regions. This electric field anomaly, also observed in charged particle measurements by *Stolzenburg and Marshall* [1998], is evidence of a highly charged bilayer that resides at the interface between the lower positive region and the main negative charge region above. Termed "benchmark charge regions," these layers were found to contain charge densities on the order of $\sim$10 nC m^{-3} [*Marshall et al.*, 1995]. However, there are not many reliable measures of charge density at this level, so the true variation around this order of magnitude of observed values is unknown. For instance, at certain times, the charge densities could be significantly higher.

[16] Let us now consider the idealized situation: there are two large charge regions with a highly charged bilayer at the interface within a rotating system high in the cloud ($\sim$4–10 km above ground) (Figure 1a). The rotation will tend to centrifuge everything outward causing a lower-pressure region to form near the axis. Let us conceive that our charged bilayer dips downward along this axis of rotation because of the slightly lower pressure (Figure 1b); this could also happen because of a downdraft or because this leads to a lower energy configuration of the electromagnetic system. As the bilayer deforms, the central negatively charged downdraft finds itself surrounded by a sheath of positively charged particles rotating with the air. The charges are carried on cloud or precipitation particles [*Brown et al.*, 1971] which, when acted on by the electric force, exert a drag force on the surrounding air. The electric force now begins to draw the positively charged particles and surrounding air inward. The uncharged air will be dragged along but will tend to filter away from the axis since it lacks the extra electric force required to keep it at smaller radii of rotation; this represents a possible mechanism for charge density enhancement closer to the axis. The decrease in radius leads to a faster rotation through conservation of angular momentum. This elevated velocity will then lead to a pressure decrease in the sheath due to Bernoulli's principle. Since the contraction is happening at all radial distances outside of the core, this lower pressure will also pull outward on the core in all directions ultimately leading to a lower axial pressure. This lower axial pressure will then allow more negatively charged air to descend from above (Figure 1c), which will in turn continue to draw in charged particles in the sheath through the electric force.

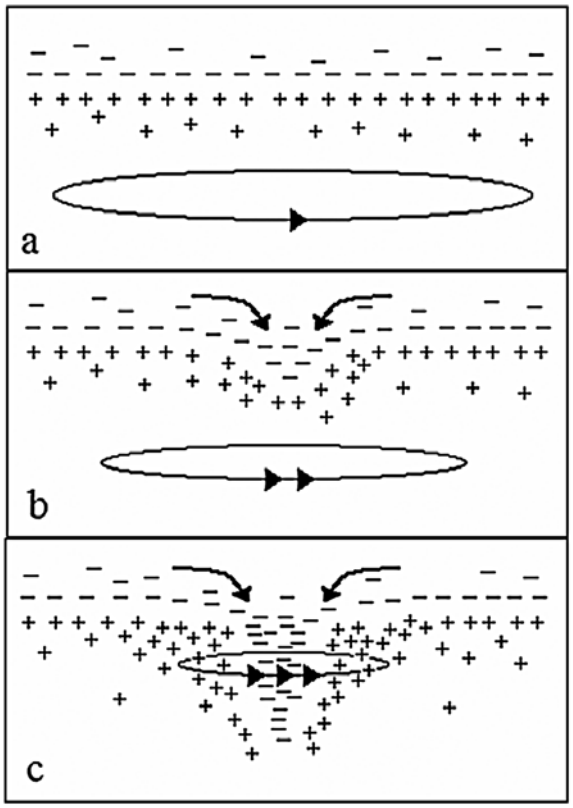

Figure 1. The series shows the progression from the benchmark charge region rotating (arrows with ring) (a) with the storm initiating at $\sim$4–10 km above ground, (b) to a central low-pressure dip, and finally (c) the attraction of positive to negative resulting in the concentration of angular momentum.

[17] The charges of the negative core will be pulled outward by the electric force but this will not decrease the amount of charge at the core. Mixing of air from the sheath and the core will occur at the boundary causing charge

neutralization, latent heating, and then removal of the mixed air from the system by being buoying upward and outward (with no electric force on the parcel after charge neutralization). This however does not stop the charge flow. In fact, the exit of this air from the system will help drive the flow because the neutralized air lost from the system will make way for more charged air from the upper layer and the sheath to flow toward the interaction region.

[18] Another important process occurring to maintain the coherence of the nascent cloud-level tornado vortex is latent heating. The ''benchmark charge regions,'' as well as charge bilayers in other thunderstorms, exist just above the altitude where the temperature crosses zero. This means that the lower positive layer likely contains water in a mixed phase ($\sim$0 to -5°C) while the upper negative layer is made up of ice particles (~-5 to -10°C and lower). When the cold air moves down the center and then mixes with the incoming sheath air, the liquid water of the sheath will completely freeze releasing its latent heat to the surrounding parcel of air. This heating will buoy the parcel upward and outward. The exiting air will not collide with the downdraft because when it heats it becomes less dense and will be pushed away from the axis of rotation. The core downdraft will be resupplied from above and the lower air has a large reservoir of rotating air that can move inward to maintain the exchange. The central downdraft remains at the low pressure of its initial level because of the intense rotation of the tornado vortex which allows the core temperature to also remain at the same degree as above. This is a very similar situation to what happens at ground level as will be discussed later.

[19] As the negative central downdraft delves deeper into the positive region the attraction of opposite charges as well as latent heating contracts the preexisting angular momentum at each successive level, this leads to a lower axial pressure through the process described above, drawing down more negatively charged air from above, which again contracts the angular momentum of the rotating positive sheath at the next lowest level. This runaway reaction will accelerate the rotation near the axis and build the cloud-level tornado vortex downward. It represents a plausible threshold scenario in which the amount of charge separation and water content determines the rate at which the tornado vortex can grow.

[20] A major prediction of this theory is that of a central downdraft originating from the cold low pressure negatively charged mid to upper levels of the storm reaching to the ground. The intense rotation of the tornado vortex ensures that the downdraft keeps a constant pressure high in the cloud to ground level. The pressure throughout the column would be slightly lower than that of the high-level air to maintain the downward movement. The continuity of the downdraft ends when the vortex ceases to rotate enough to maintain the low-pressure core. A good analogy to this is the way air reaches through the core of a bathtub drainage vortex: the air is much less dense than the water but the rotation creates a low enough axial pressure to support the flow. In the drainage case, the exchange of air along the axis facilitates the faster drainage of the water reinforcing the flow and intensifying the water vortex. While there are no direct in-cloud measurements of the hypothesized low-pressure core, there is some evidence for its existence.

[21] Descending TVS data from *Trapp et al.* [1999] shows that radar images of intense tornado vortices are connected from high in the cloud to the ground while tornadoes are on the ground (peak velocities measured aloft $>2-7$ km before ground-level tornadogenesis). The axial pressures within these vortices must be lower than outside them at any given height level. Thus, if the intense rotation extends from the freezing level (anywhere between 3 and 8 km) downward, as the evidence shows it does, then there exists a possible low-pressure conduit that could transport this high-level air downward. Therefore, although it may occur in a minority of systems, there is a plausible configuration whereby air from freezing levels is connected through a low-pressure vortex with the ground.

[22] As stated earlier, few electrical measurements exist in this region of the storm, but it seems reasonable that charge densities in these systems may have a large range of values. This range will be further expanded in the system discussed because of the suggested charge density enhancement mechanism. Systems with insufficient charge density to induce a strong enough electrical force or not enough rotation will fail to develop beyond their embryonic stage. Systems with too much charge density will simply discharge through lightning. It is therefore beneficial to attempt to understand what this charge density threshold is in a quantitative manner.

6. Electric Versus Centripetal Force Comparisons and a Time Estimate

[23] The following calculation represents an estimate of the electrical force in a developing tornado vortex high in the cloud (as measured as a TVS) in comparison with the centripetal force. The hypothesis is that the electrical component of some developing tornadoes might serve as a catalyst for intensification. This simple analytical model assumes the charge distribution is given by two concentric cylinders with the negative charges residing in the core and the positive charges distributed throughout the outer cylinder. We assume the cylinders have inner radius a and outer radius b, all negative charges are in $r < a$, and all positive charges live in $a < r < b$ (r is the distance from the core center). Furthermore, for simplicity we assume the electric field outside of the cylinders $r > b$ is zero, so that the total amount of positive charges in the outer cylinder is strictly fixed by the amount of negative charges in the inner cylinder.

[24] Since the proposed mechanism by which electrical forces contribute to genesis primarily deals with the ability of the negative core to attract the positive outer charges, the relevant region for the estimate is $a < r < b$. By Gauss's law, the actual distribution of negative charges, ρ_-, is irrelevant if we assume cylindrical symmetry; only the total charge enclosed contributes to the electrical field. Thus, assuming a uniform charge distribution,

$$Q_{encl}^{(-)} = \int_0^a r\rho_- dr d\phi dz = a^2 \pi L \rho_- \ , \qquad (1)$$

where L is the length of the cylinder. Using a = 500 m and $\rho_- = -20$ nC m^{-3}, the total charge enclosed per vertical length in the core is

$$\frac{Q_{encl}^{(-)}}{L} = a^2\pi\rho_- = -\pi\left(250000\ m^2\right)\left(20\times10^{-9}C/m^3\right) = -1.57\times10^{-2}\ C/m. \quad (2)$$

[25] The highest measured benchmark charge regions from *Marshall et al.* [1995] were 13.4 nC m^{-3} and the highest inferred charge density from measurements of a multicell severe thunderstorm by *Byrne et al.* [1987] was -17 nC m^{-3}. Therefore, a core charge density of $\rho_- \approx -20$ nC m^{-3} is a reasonable estimate of what can occur in a supercell (and of course, higher values are possible).

[26] In order to justify our estimate of the core radius being 500 m we will use the definition of a TVS. A TVS is when a radar measures greater than 15 m/s change in gate-to-gate velocity. From *Trapp et al.* [1999] the average distance from the radar to all descending tornado vortices measured as TVSs was 78 km. Using a radar radial resolution of 1 degree we find that this corresponds to a TVS diameter of 1.36 km (from the middle of one gate to the middle of the next one). Our adoption of 500 m as the inner radius is therefore consistent with this data. For the outer radius, b, we adopt a value of 1500 m as this represents a plausible diameter for observed mesocyclones.

[27] We will initially assume a quadratic distribution of positive charges in the outer cylinder. The positive charge distribution, ρ_+ is constrained by the following requirements: (1) $\rho_+(a) = \rho_+(b) = 0$. (2) The maximum in the charge density is fixed so that the spatially integrated positive charge density (i.e., total charge) is equal to the total charge enclosed in the negative core.

[28] For charge neutrality outside the system, we have:

$$\int_0^a r\rho_- dr d\phi dz + \int_a^b r\rho_+(r) dr d\phi dz = 0, \quad (3)$$

with ρ_- given above, and ρ_+ a parabolic distribution centered at *(a + b)/2*:

$$\rho_+(r) = A\left(r - \frac{1}{2}(a+b)\right)^2 + B. \quad (4)$$

[29] Using the first constraint above, we have

$$\rho(r=a,b) = 0 = A\left(\frac{a-b}{2}\right)^2 + B \rightarrow B = -\frac{1}{4}(a-b)^2 A, \quad (5)$$

which gives a positive charge distribution of

$$\rho_+(r) = A\left[r^2 - (a+b)r + ab\right], \quad (6)$$

with A determined by constraint number 2 (i.e., equation (3)):

$$\frac{Q_{encl}^{(-)}}{L} = -2\pi\int_a^b r\rho_+ r dr. \quad (7)$$

[30] Substituting for the explicit charge distribution, performing the integral, and solving for A, we find:

$$A = \frac{6Q_{encl}^{(-)}}{\pi L(b^2-a^2)(b-a)^2} = \frac{6a^2\rho_-}{(b^2-a^2)(b-a)^2}. \quad (8)$$

[31] Entering the values a = 500 m, b = 1500 m, and $\rho_- = -20$ nC m^{-3}, we find:

$$A = -1.5\times10^{-14}\ C/m^5$$
$$B = 3.7\times10^{-9}\ C/m^3 \quad (9)$$

which gives

$$\rho_+(r) = -1.5\times10^{-14}\ C/m^5\left[r^2 - (2000m)r + \left(750000m^2\right)\right]. \quad (10)$$

[32] Using this in Gauss's law gives the electrical field as a function of r in the region $a < r < b$:

$$E(r) = \frac{1}{2\pi r L\varepsilon_0}\left(Q_{encl}^{(-)} + \int_a^r \rho_+(r')r' dr' d\phi dz\right). \quad (11)$$

[33] Performing the integration, the electric field obtains the form:

$$E(r) = \frac{\alpha}{r} + \beta r + \gamma r^2 + \delta r^3, \quad (12)$$

where

$$\alpha = \frac{a^2b^3\rho_-}{2\varepsilon_0}\frac{(b-2a)}{(b^2-a^2)(b-a)^2} = -2.38\times10^8\ Nm/C \quad (13)$$

$$\beta = \frac{Aab}{2\varepsilon_0} = -636\ N/Cm \quad (14)$$

$$\gamma = \frac{-A(a+b)}{3\varepsilon_0} = 1.13\ N/Cm^2 \quad (15)$$

$$\delta = \frac{A}{4\varepsilon_0} = -4.24\times10^{-4}\ N/Cm^3 \quad (16)$$

[34] From the electric field, we can determine the corresponding magnitude of force/mass of a test charge:

$$F_{EM}/m = qE/m. \quad (17)$$

[35] Now we determine the distance r from the core's center at which the electrical force is of the same order of magnitude as the centripetal force,

$$F_{cent}/m = v^2/r = r\omega^2, \quad (18)$$

where v is the velocity of the charges at r, ω is the angular velocity, and we assume that $v = r\omega$, with ω approximately constant throughout the cylinder. To estimate ω, we assume

a gate-to-gate velocity of 15 m/s (that is 7.5 m/s toward an observer and 7.5 m/s away) at a radius of 680 m, consistent with the definition of a TVS and observations [*Trapp et al.*, 1999]. This gives $\omega = 0.011\ s^{-1}$. So

$$\left|\frac{qE}{m}\right| \sim |r\omega^2| \tag{19}$$

gives a polynomial equation for r:

$$\delta r^4 + \gamma r^3 + \xi r^2 + \alpha = 0, \tag{20}$$

where

$$\xi = \beta + \frac{\omega^2}{q/m} = -480\ N/Cm, \tag{21}$$

assuming a test charge with charge $q = 3 \times 10^{-11}$ C and mass $m = 3.88 \times 10^{-5}$ kg (the origin of these values is explained in the paragraph below). The + sign in the equation from ξ comes from the fact that the electric force is negative in the region $a < r < b$, so when equated to a positive number, there must be an overall $(-)$ sign. Plugging in all of the numbers and solving the polynomial numerically gives one relevant value for r: 1016 m. Using $r = 1000$ m to estimate the forces, we find $F_{EM}/m = 0.13\ m/s^2$ and $F_{cent}/m = 0.12\ m/s^2$. Thus, where the peak of the positive charges is, the electrical force is on the order of the centripetal force. For charges closer than 1000 m (but greater than a), the electrical force is a viable candidate for a ''trigger'' mechanism in tornadogenesis, while for distances greater than this the effect is diminished. Since the ''peak'' of the positive charges is at 1000 m, a significant portion of positive charges will be attracted to the negative core, in this model.

[36] The biggest uncertainty in this approach lies in our estimate of the charge on the test particle. No data exists (to our knowledge) on either the size or charge of particles (water droplet, hailstone, graupel, etc) within supercells where tornadoes form. It has been shown however, that different types of thunderstorms (New Mexican thunderstorms, Mesoscale Convective Systems, and Supercells) have the same basic charge structures [*Stolzenburg et al.*, 1998b]. The same researchers found that highly charged layers in the weak updraft region of New Mexican thunderstorms are very similar in charge density to the benchmark regions found by *Marshall et al.* [1995] and even have the same temperature profile. Also, both studies indicated that the lower layer's charge is carried on precipitation particles. For these reasons we assume that the particle size and charge found on individual particles in the New Mexican thunderstorm should be similar to those found in analogous layers in a typical supercell; the difference in a supercell would be that the spatial extent is larger and the system is rotating. *Stolzenburg and Marshall* [1998] reported a mean single positive particle charge in the layer between 6 and 6.6 km height (analogous to Marshall et al.'s benchmark region) as being 29.3 pC. We therefore use an estimate of 30 pC for the charge on our orbiting particle. *Stolzenburg and Marshall* [1998] also report an average droplet diameter of 2.1 mm. Using this diameter and the density of water we can estimate the mass of these particles (assuming a spherical shape) leading to the estimated mass of 3.88×10^{-5} kg.

[37] This approach is synthetic in the sense that there are not such sharp separations between charge regions or constant densities. As a result this approach creates an edge effect of a high electric field. As a second possible charge configuration that may be closer to reality we will now consider an exponential charge density distribution in the positive region:

$$\rho_+ = Ae^{-Br} + C, \tag{22}$$

subject to the boundary conditions:

$$\begin{aligned} \rho_+(a) &= 20 \times 10^{-9} C/m^3 \equiv \rho_a \\ \rho_+(b) &= 1 \times 10^{-9} C/m^3 \equiv \rho_b \end{aligned} \tag{23}$$

[38] These boundary conditions give

$$A = \frac{\rho_a - \rho_b}{e^{-Ba} - e^{-Bb}}, \tag{24}$$

$$C = \frac{\rho_b e^{-Ba} - \rho_a e^{-Bb}}{e^{-Ba} - e^{-Bb}}. \tag{25}$$

[39] The decay rate is given by B, and is determined by the assumption that we have charge neutrality outside the cylinders:

$$\int_a^b \rho_+(r)dr = -a^2\rho_-/2, \tag{26}$$

where the negative charge density of the core is assumed to be a constant.

[40] Inserting the exponential charge distribution into the condition of charge neutrality gives:

$$\frac{A}{B}\left\{(b + 1/B)e^{-Bb} - (a + 1/B)e^{-Ba}\right\} = a^2\rho_-/2 + C\left(b^2 - a^2\right)/2. \tag{27}$$

Plugging in the expressions for A and C gives an equation for B:

$$e^{-B(b-a)} = \frac{\frac{\rho_a - \rho_b}{B}(a + 1/B) + a^2\rho_-/2 + (b^2 - a^2)\rho_b/2}{\frac{\rho_a - \rho_b}{B}(b + 1/B) + a^2\rho_-/2 + (b^2 - a^2)\rho_a/2}. \tag{28}$$

Plotting both sides of the equation as a function of B, we find they intersect at a value close to:

$$B = 7.9 \times 10^{-3} m^{-1}. \tag{29}$$

For this value of B, the left and right hand sides of equation (28) give 3.71×10^{-4} and 3.26×10^{-4} respectively. Newton's method would have given a closer approximation, but given that we are interested in orders of magnitudes and

the error bars are already large, we simply used the value of B above. Given B,

$$A = 9.87 \times 10^{-7}\ C/m^3, \tag{30}$$

$$C = 9.93 \times 10^{-10}\ C/m^3. \tag{31}$$

[41] Again using Gauss's Law to determine the electric field in the region $a < r < b$, we find

$$E = \frac{\alpha}{r} + \beta r + \frac{\gamma}{r} e^{-Br} + \delta e^{-Br}, \tag{32}$$

with

$$\alpha = \frac{a^2 \rho_-}{2\varepsilon_0} + \frac{A}{\varepsilon_0 B}(a + 1/B)e^{-Ba} - \frac{Ca^2}{2\varepsilon_0} = -1.26 \times 10^8\ Nm/C \tag{33}$$

$$\beta = \frac{C}{2\varepsilon_0} = 56.1\ N/mC \tag{34}$$

$$\gamma = -\frac{A}{\varepsilon_0 B^2} = -1.79 \times 10^9\ Nm/C \tag{35}$$

$$\delta = -\frac{A}{\varepsilon_0 B} = -1.41 \times 10^7\ N/mC \tag{36}$$

[42] Again, comparing the magnitudes of the electrical force per mass, $F_{EM}/m = qE/m$ with the centripetal force per mass $F_{cent}/m = r\omega^2$, we find the values of Table 1. Since a majority of the positive charges live in the region $a < r < 800$ m for the assumed exponential charge distribution, this further reinforces the possibility that the electrical force is a plausible "trigger" mechanism for tornadogenesis. This trigger is dependent on the actual charge density and our models show that for values of $\rho_- = -20$ nC m^{-3} or above, the electrical force per particle is 0.5–1.0 times that of the centripetal force on uncharged air. Thus, through force addition, this potential effect is likely part of the real physics of tornadogenesis.

[43] Now we will attempt to use the theorized flow structure to get a time estimate for cloud-level tornado vortex contraction. As an ideal model, we have assumed a static core cylinder of negative charge at the center around which a sheath of positive charge rotates at a constant rate. To simplify this model further, we will consider only a single charged particle rotating around the core at some initial radius. If there were no charges on either body then the rotating particle will remain in orbit around the core at the same radius because of the pressure gradient force; we neglect any turbulent effects for now. With the addition of charges there will be an imbalance of forces and the charged particle will be drawn inward. The balance of forces then reduces to a one-dimensional equation with radial forces:

$$ma = \frac{\rho_- R^2 q_+}{2\varepsilon_0 r} - \frac{\rho_{air} A C_D v^2}{2} \tag{37}$$

Table 1. Force Comparison With Exponential Distribution[a]

	r = 500 m	r = 800 m	r = 1000 m
$F_{EM}/m = qE/m$	0.44	0.11	0.06
$F_{cent}/m = r\omega^2$	0.06	0.10	0.12

[a]Units are m s^{-2}.

where the first term on the right is the electric force that a uniform cylindrical volume of charge has on a charged particle at some radial distance, and the second term is the drag force of a particle moving through the air dependent on the square of its velocity. The notation is as follows:

- ρ_- the charge density in the central downdraft;
- R the radius of the cylindrical core;
- q_+ the charge on the single orbiting particle;
- m the mass of the orbiting positive particle;
- r the current radial position of the orbiting particle from the axis;
- ε_0 the permeability of free space;
- ρ_{air} density of air;
- C_D drag coefficient;
- A the cross-sectional area of the particle;
- v radial velocity of the particle;
- a the acceleration of the particle.

[44] We solve for acceleration and then are able to numerically integrate twice to find position as a function of time. With a time-dependent position, we can estimate the time it takes for the particle to reach the outer radius of the core. We do this by starting the particle from rest, calculating the instantaneous acceleration, allowing the particle to accelerate at that rate for one time step, and then recalculating the acceleration and velocity. Repeatedly stepping through this routine, we track the radial position of the charged particle, radial velocity, time, and acceleration. For our model the time step was set to one second; making it smaller did not change the resulting contraction time appreciably. Other variables listed above were given realistic values, based on available observations, and will be explained presently.

[45] As discussed above, a core charge density of $\rho_- \approx -20$ nC m^{-3} is a reasonable estimate of what really occurs in a supercell. For the purpose of this estimate we will allow the core charge density to range from -0.1 nC m^{-3} to -20 nC m^{-3}. The estimate of charge on our single particle will be the same as that above: 30 pC. Furthermore, the average droplet diameter of 2.1 mm will be used along with the density of water to get an estimate of the mass and the cross-sectional area of the particle.

[46] Positively charged particles will start at some radius from the axis of the supercell rotation and "fall" inward to the final (core) radius. We will set the beginning radius to be 3000 m (consistent with a large-scale mesocyclone) and we will set the final core radius to be 500 m as above. Also we assume $\rho_{air} = 1$ kg m^{-3} and $C_D = 1$ (due to estimates of the Reynolds number associated with our moving particle).

[47] If we use these estimates of the physical parameters in combination with the force balance equation derived above, we can derive a relation between core charge density and particle transit time. Figure 2 shows that the time needed for a charged particle to move from 3 km to $^1/_2$ km, in minutes, is consistent with timescales measured TVSs form on.

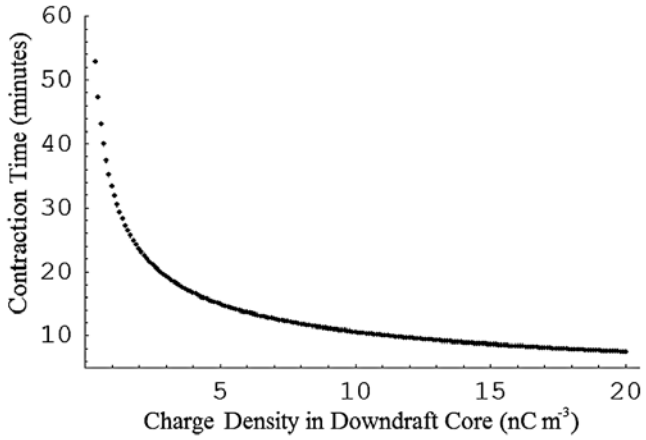

Figure 2. The time dependence of a particle to reach the core radius as a function of central down draft charge density.

[48] If we arbitrarily state that any angular contraction that takes more than ~15 min will fail to develop because of turbulent dissipation then we can say that any core charge densities higher than ~5 nC m^{-3} indicate a high probability of cloud-level tornado vortex formation, TVS measurement, and high tornado danger. This statement must be tempered by the fact that supercells with a highly coherent large-scale rotation will be able to form cloud-level tornado vortices on longer timescales, while more turbulent cells will not remain stable long enough for the contraction of preexisting angular momentum to fully mature. This indicates that there should be some parameter space in which charge density and cloud rotation can predict the probability of cloud-level tornado vortex formation. This is well beyond the scope of this calculation and model and is left for future investigation. Overall, however, our model and calculation has returned a contraction timescale that is consistent with storm timescales. This fortifies our main scientific point: once the charge density reaches a critical value, there is a significant probability that tornadogenesis will occur.

[49] The force comparisons and time estimate for a charged particle to move to the outer core show that the contraction of preexisting angular momentum through the electric force could be a possibility in the midaltitudes of the supercell. Let us now examine the arrival and behavior of this type of flow structure at ground level.

7. Ground-Level Tornadoes and Latent Heating

[50] Once the nascent tornado has formed in the cloud as a tornado vortex and is measurable as a TVS, the runaway process explained above will build the vortex downward until either the reaction runs out of energy (either rotational, charge separation, or latent heating energy) and decays, or the vortex reaches close enough to the ground to tap into the massive convective available potential energy (CAPE); the CAPE number represents the energy density of moist air if all the water were condensed and the energy released via latent heating. It has been found that enhanced levels of CAPE, as well as boundary layer shear (rotation in the lowest 6 km of a supercell measurable by radar), are present at the time of tornado formation [*Rasmussen and Blanchard*, 1998]. Typical values of CAPE at the ground near tornadoes average 1300 J kg^{-3} but can be up to around 3000 J kg^{-3}. The values of boundary layer shear near where tornadoes have formed have been found to be around 18 m s^{-1} on average with a maximum of 29 m s^{-1} [*Rasmussen and Blanchard*, 1998].

[51] Introduction of a descending tornado vortex with a cold low-pressure central core (on the order of −10°C) into an area with large CAPE and sufficient boundary layer shear will form a ground-level tornado. When the cold air core of a tornado vortex reaches low enough to come into contact with air containing a lot of moisture then this may be a ''sudden'' source of energy that can act as a trigger. As the ground-level air makes its way toward the axis of the tornado vortex it will lose its heat as a result of the core's temperature until it reaches the freezing point. The subsequent latent heating could occur immediately leading to a violent upwelling from near ground levels. The influence of the electric force near ground level will range from large to small depending on the local conditions, but it seems that latent heating will always be the dominant process at this level.

[52] Latent heating leads to a stable flow because the preexisting shear of the ground-level air ensures the continuity of the system. As the heated air moves upward because of the release of CAPE, the ground-level moist air is pulled inward to replace it and will be forced into orbit around the core because of conservation of angular momentum. This orbiting moist air will then mix with core air, heat due to the release of CAPE, and then move upward quickly. This reaction allows the central downdraft to remain intact while keeping the pressure at the axis of rotation low enough to facilitate the continual descent of the cold core. The air of the cold downdraft is continually lost to mixing with the ground-level air, but it will also be replaced continually from the reservoir above. This geometry is stable as long as both air reservoirs are not depleted.

[53] For clarity, the destructive intensity of the winds at the ground is most likely a local enhancement due to the boundary condition that the velocity must be zero at the ground and corner flow dynamics as suggested by *Lewellen et al.* [1997] and *Lewellen and Lewellen* [2007]. Our theory lays out the flow development and final configuration which leads to an intense hydrodynamic axial sink.

[54] This configuration can also explain the long life of single tornadoes or multiple track tornadoes. A single tornado can exist for a long time as long as the conditions are favorable to maintain the reaction. Conversely, if the ground-level air runs out of enough CAPE to continue the reaction, or the tornado entrains too much mass to rotate fast enough to maintain the low-pressure core, the ground-level tornado can break up and ascend into the clouds only to return minutes (or tens of minutes) later when more CAPE is available or the rotation has simply rid itself of the debris it was carrying; the cloud-level tornado vortex never stops its rotation. Assuming that charge exchange continues to fuel the tornado vortex in the cloud, the ground-level tornado can persist as long as the storm continually moves through areas with high ground-level CAPE.

[55] This type of ground-level tornadic flow is known as a ''two-celled'' structure (a central downdraft with an upward moving outer sheath) and has been suspected for many years [*Davies-Jones*, 1986; *Whipple*, 1982]. Stable solutions to the Navier-Stokes equation with this geometry have been pre-

sented [*Kuo*, 1966; *Sullivan*, 1959]. Furthermore, an echo free region (i.e., free of liquid hydrometeors) at the core of larger tornadoes is known to exist and has been directly observed through the use of the Doppler On Wheels (DOW) [*Bluestein et al.*, 2003; *Wurman*, 2002]. Our theory goes one step further by plausibly explaining the development of the central downdraft and formation of the tornado vortex.

[56] Another possible scenario occurs when enough ground-level boundary layer shear and enough CAPE exists that the rotation may be able to create an intense ground-level vortex similar to a dust devil. This mode of formation may be more short lived as it will not have the stabilizing effect of the electric force from the cloud above, but it can still have devastating wind speeds. This is probably a good explanation as to what happens in mode II TVS tornadogenesis when the tornado starts near the ground or forms throughout many kilometers of storm simultaneously. Indeed, viable numerical models have demonstrated tornado-like behavior without the presence of any electric forces [*Lewellen et al.*, 1997; *Wicker and Wilhelmson*, 1995].

8. Discussion

[57] With the presence of sufficient rotational energy in the pretornadic mesocyclone to accelerate air to tornado vortex speeds, we have presented a novel theory that suggests an electrical mechanism plays a crucial role in allowing the cloud-level contraction of preexisting rotation. Cloud-level tornado vortices would occur when enough rotational coherence is coupled with the required charge separation. Through consideration of the organizing role of charge density, we have outlined a plausible runaway effect for accelerating and sustaining a rotating column of air building from upper cloud levels toward the ground. This situation likely occurs when there is substantial charge in the cloud but not enough to discharge the buildup through lightning. We have further shown in simplified models that observed charge densities lead to inward forces that rival and sometimes dominate the required centripetal force and can lead to plausible contraction timescales for tornado vortices. We have further presented a plausible explanation for ground-level tornadic stability. A natural result of the proposed geometry is that latent heating leads to a hydrodynamic sink sustaining the concentration of angular momentum at ground level as well as keeping the axial pressure low enough to continually draw down cold air from above.

[58] The suggested geometry has three specific testable attributes: (1) significant central negative charge density, (2) a horizontal temperature profile above the ground with strong transition regions between warm and cold air, and (3) a low-pressure core.

[59] The first attribute may only be testable away from ground level since as the core descends its charges will migrate outward toward the sheath and neutralize. Lightning holes may be evidence of this configuration but are not understood well enough yet to be used as conclusive proof.

[60] The second attribute is more easily probed near ground level. The horizontal temperature cross section of a tornado above the ground will look something like

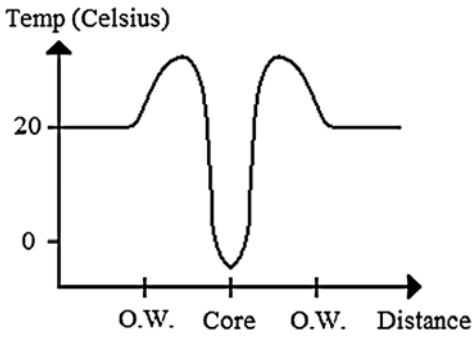

Figure 3. Theoretical temperature profile through the core of a tornado. O.W. means outer wall where water is condensed releasing latent heat.

Figure 3 (the levels are not meant to be exact, but represent the general trends that will be observed).

[61] The heated mixing regions where CAPE is being released are represented by the two upward bumps and should be warmer than both the core and the ambient. The cool core is at the center and should be colder than the freezing point of water. Outside of the heated bumps the temperature approaches ambient conditions. The resolution of this cross section is worse closer to the ground because of boundary layer turbulence. The best measurement will come from a large tornado with good ground contact ensuring the presence of a substantial core near the ground that sustains itself for a few minutes.

[62] The third measurable parameter is pressure and should be measurable near ground level. Our model has a core reaching the ground that is pulling air from high cloud levels. Therefore, the pressure in the core should be the same as that of where the air is originating. This means that the core pressure near ground level should be less than half that of the ambient ground-level pressure. The pressure right at the ground will be subject to boundary layer conditions and therefore must be a mix of ground-level and high-level air. Therefore, the core pressure right at ground level will depend on the diameter of the tornado at the ground and how well the core is screened from the ambient pressure by the rising walls of the tornado. The pressure deficit will be most easily measured in large long-lived strong tornadoes.

[63] Indeed, *Winn et al.* [1999] have observed a steeper than previously predicted pressure decline with radius at the ground near a large tornado. Unfortunately, on axis measurements were not possible. This indicates that axial pressures may be much lower than previously thought possible. Interestingly, the instrument that was closest to the center of the tornado but which was still outside the core (probably in the sheath) did show a higher potential temperature than the other instruments at the time the tornado passed [*Winn et al.*, 1999]. These findings may point to sheath heating due to the release of CAPE, however this is only one measurement and we must seek more data to verify such a conclusion.

[64] Tornadoes are very complex highly nonlinear systems which certainly contain one of the highest energy densities of any natural system in the world. It is precisely because of these energetic conditions that instrument measurement of the details of these systems is difficult. In particular, a

tornado has a natural Reynolds number of $\sim 10^8$ which will shred most instrumental attempts at measurement. Thus, our knowledge of the detailed physics in these systems is quite limited which in turn limits our understanding of the various trigger mechanisms for tornadogenesis; which in turn limits our predictive ability. The model presented here suggests that under certain conditions, increasing amounts of charge density can become a viable mechanism for the dominant type of tornadogenesis in supercells. We hence suggest that continued efforts to measure the overall electrical properties of these systems can and will lead to new insight into their formation and evolution.

[65] **Acknowledgments.** We thank Nikki Bowen, Brian Smith, Daniel DePonte, Alan VanDrie, and Geri Infante for many discussions and support. We would like to thank the two anonymous reviewers for their helpful thoughts and advice which have made the paper better. We further thank Stephen Kevan for understanding that there is more to life than condensed matter physics.

References

Bacon, F. (1844), Natural history of winds—Extraordinary winds and sudden blasts, in *The Works of Francis Bacon*, pp. 449–452, Carey and Hart, Philadelphia, Pa.

Bluestein, H. B., C. C. Weiss, W. C. Lee, M. Bell, and A. L. Pazmany (2003), Mobile Doppler radar observations of a tornado in a supercell near Bassett, Nebraska, on 5 June 1999. Part II: Tornado-vortex structure, *Mon. Weather Rev.*, *131*(12), 2968–2984.

Brown, K. A., P. R. Krehbiel, C. B. Moore, and G. N. Sargent (1971), Electrical screening layers around charged clouds, *J. Geophys. Res.*, *76*, 2825–2835.

Brown, R. A., L. R. Lemon, and D. W. Burgess (1978), Tornado detection by pulsed Doppler radar, *Mon. Weather Rev.*, *106*, 29–39.

Byrne, G. J., A. A. Few, M. F. Stewart, A. C. Conrad, and R. L. Torczon (1987), In situ measurements and radar observations of a severe storm: Electricity, kinematics, and precipitation, *J. Geophys. Res.*, *92*, 1017–1031.

Church, C. R., and B. J. Barnhart (1979), A review of electrical phenomena associated with tornadoes, paper presented at 11th Conference on Severe Local Storms, Am. Meteorol. Soc., Kansas City, Mo.

Davies-Jones, R. P. (1986), Tornado dynamics, in *Thunderstorm Morphology and Dynamics*, edited by E. Kessler, pp. 197–236, Univ. of Okla. Press, Norman.

Davies-Jones, R., R. J. Trapp, and H. B. Bluestein (2001), Tornadoes and tornadic storms, in *Severe Convective Storms*, *Meteorol. Monogr.*, vol. 50, pp. 167–221, Am. Meteorol. Soc., Boston, Mass.

Hare, R. (1837), On the causes of the tornado or waterspout, *Am. J. Sci. Arts*, *32*, 153–161.

Krehbiel, P., T. Hamlin, Y. Zhang, J. Harlin, R. Thomas, and W. Rison (2002), Three-dimensional total lightning observations with the Lightning Mapping Array, paper presented at 2002 International Lightning Detection Conference, Global Atmos., Inc., Tucson, Ariz.

Kuo, H. L. (1966), On the dynamics of convective atmospheric vortices, *J. Atmos. Sci.*, *23*, 25–42.

Lang, T., et al. (2004), The severe thunderstorm electrification and precipitation study, *Bull. Am. Meteorol. Soc.*, *85*, 1107–1125.

Lewellen, D. C., and W. S. Lewellen (2007), Near-surface intensification of tornado vortices, *J. Atmos. Sci.*, *64*, 2176–2194.

Lewellen, W. S., D. C. Lewellen, and R. I. Sykes (1997), Large-eddy simulation of a tornado's interaction with the surface, *J. Atmos. Sci.*, *54*(5), 581–605.

Lucretius, C. T. (1950), *De Rerum Natura*, 260 pp., E. P. Dutton, New York.

MacGorman, D., and W. Rust (1998), *The Electrical Nature of Storms*, Oxford Univ. Press, New York.

MacGorman, D., D. W. Burgess, V. Mazur, W. D. Rust, W. L. Taylor, and B. C. Johnson (1989), Lightning rates relative to tornadic storm evolution on 22 May 1981, *J. Atmos. Sci.*, *46*(2), 221–250.

Marshall, T. C., W. D. Rust, and M. Stolzenburg (1995), Electrical structure and updraft speeds in thunderstorms over the southern Great Plains, *J. Geophys. Res.*, *100*(D1), 1001–1015.

Peltier, J. C. A. (1840), Observations et recherches expérimentales sur les causes qui concourent à la formation des trombes, *Am. J. Sci. Arts*, *38*, 73–86.

Rasmussen, E. N., and D. O. Blanchard (1998), A baseline climatology of sounding-derived supercell and tornado forecast parameters, *Weather Forecasting*, *13*, 1148–1164.

Stolzenburg, M., and T. C. Marshall (1998), Charged precipitation and electric field in two thunderstorms, *J. Geophys. Res.*, *103*(D16), 19,777–19,790.

Stolzenburg, M., W. D. Rust, and T. C. Marshall (1998a), Electrical structure in thunderstorm convective regions: 2. Isolated storms, *J. Geophys. Res.*, *103*(D12), 14,079–14,096.

Stolzenburg, M., W. D. Rust, and T. C. Marshall (1998b), Electrical structure in thunderstorm convective regions: 3. Synthesis, *J. Geophys. Res.*, *103*(D12), 14,097–14,108.

Sullivan, R. D. (1959), A two-cell vortex solution of the Navier-Stokes equations, *J. Aerosp. Sci.*, *26*, 767–768.

Trapp, R. J., E. D. Mitchell, G. A. Tipton, D. W. Effertz, A. Watson, D. L. Andra, and M. A. Magsig (1999), Descending and nondescending tornadic vortex signatures detected by WSR-88Ds, *Weather Forecasting*, *14*(5), 625–639.

Trapp, R. J., S. A. Tassendorf, S. A. Godfrey, and H. E. Brooks (2005), Tornadoes from squall lines and bow echoes. Part 1: Climatological distributions, *Weather Forecasting*, *20*, 23–34.

Vonnegut, B. (1960), Electrical theory of tornadoes, *J. Geophys. Res.*, *65*(1), 203–212.

Vonnegut, B., and J. R. Weyer (1966), Luminous phenomena in nocturnal tornadoes, *Science*, *153*, 1213–1220.

Watkins, D. C., J. D. Cobine, and B. Vonnegut (1978), Electrical discharges inside tornadoes, *Science*, *199*, 171–174.

Whipple, A. B. C. (1982), *Storm*, Time-Life Books, New York.

Wicker, L. J., and R. B. Wilhelmson (1995), Simulation and analysis of tornado development and decay within a three-dimensional supercell thunderstorm, *J. Atmos. Sci.*, *52*, 2675–2703.

Winn, W. P., S. J. Hunyady, and G. D. Aulich (1999), Pressure at the ground in a large tornado, *J. Geophys. Res.*, *104*(D18), 22,067–22,082.

Winn, W. P., S. J. Hunyady, and G. D. Aulich (2000), Electric field at the ground of a large tornado, *J. Geophys. Res.*, *105*(D15), 20,145–20,153.

Wurman, J. (2002), The multiple-vortex structure of a tornado, *Weather Forecasting*, *17*(3), 473–505.

Zhang, Y., Q. Meng, P. R. Krebiel, X. Liu, and X. Zhou (2004), Spatial and temporal characteristics of VHF radiation source produced by lightning in supercell thunderstorms, *Chin. Sci. Bull.*, *49*(6), 624–631.

G. D. Bothun and F. S. Patton, Department of Physics, University of Oregon, Eugene, OR 97403, USA. (forestp@gmail.com)

S. L. Sessions, Department of Physics, New Mexico Institute of Mining and Technology, Socorro, NM 87801, USA.